Water Qual. monitoring
Temp
Plant
PI Riv Temp survey
Appendix not attached
Ref Water Qual
Ice
L. Pepin
for Appendix

RESIDUAL HEAT INPUT FROM THE MISSISSIPPI RIVER TO LAKE PEPIN DURING THE WINTERS OF 1981/82 TO 1985/86

by

H. G. Stefan

September 1987

TABLE OF CONTENTS

1. INTRODUCTION

The residual heat content of the Mississippi River at its inflow to Lake Pepin became an issue when Northern States Power Company was issued a permit to operate the Prairie Island nuclear power generating plant in a once-through cooling water cycle during the winter months. The plant discharges and rejects cooling water into the Mississippi River about 12 miles upstream from Lake Pepin. The cooling water becomes mixed with the river and the waste heat from the powerplant, along with any natural heat, is dissipated to the atmosphere as the river flows from the plant site through Dam No. 3 towards Lake Pepin. The process of heat rejection to the atmosphere depends on weather, river flow, and the amount of waste heat received, and is not necessarily completed when the Mississippi River enters Lake Pepin.

Lake Pepin is a natural widening of the Mississippi River into a lake-like basin. It has been used for winter recreational activities, particularly ice-fishing. Because the residual heat input to the lake from the Mississippi River might affect ice covers, and hence the safety of people on the lake in winter, NSP has been monitoring water temperatures and ice thicknesses in Lake Pepin during the last several winters.

The observed lake data need to be related to the river heat content, including the waste discharge, to determine if further monitoring of Lake Pepin is necessary in the future. As a first step, measured river flows and water temperatures at Dam No. 3 have been related to weather data to determine the residual waste heat content in the Mississippi River upon entering Lake Pepin. Enough daily data have been analyzed to estimate the frequency distribution of water temperatures at the inflow to Lake Pepin (Lake Pepin Delta). The inflow data can be related to stratified flow conditions in Lake Pepin in the winter to determine the impact of the river flow (carrying the residual heat) on lake ice cover.

In this report, the moments and the frequency of waste heat residuals in the Mississippi River upon entering Lake Pepin are determined and their effect on lake ice covers in winter is inferred. Since no direct Mississippi River water temperatures in the Lake Pepin delta are available, the Mississippi River heat content at that location has been calculated from weather conditions and flow rates and water temperatures at Lock and Dam No. 3. Daily weather conditions observed from December through March of the years 1981 to 1986 have been used and frequencies of calculated daily inflow water temperatures have been determined.

2. HEAT TRANSPORT IN THE RIVER

In this study, the water temperatures in the Mississippi, with artificial heat input from the Prairie Island power plant, have been calculated for winter conditions. The heat discharged into the river is advected downstream by the flow and eventually transferred to the atmosphere by radiation, evaporation and convection. Thus, the temperature distribution downstream from the point of thermal discharge depends on the hydrodynamic characteristics of the stream and the meteorological conditions prevailing at the site. The heat transfer at the soil-water interface, being small, is neglected. The river cross-section is assumed to be constant. A quasi-steady state approach is used for predicting temperatures. The river is assumed to be well mixed across the cross section. The residual heat content in the Mississippi water at its entrance to Lake Pepin is obtained.

The one-dimensional equation for heat transport in a river of constant cross-sectional area is given by

$$\frac{\delta T}{\delta t} + u\,\frac{\delta T}{\delta x} - E\,\frac{\delta^2 T}{\delta x^2} = \frac{S(T)}{\rho c_p h} \tag{2.1}$$

where
- u = average flow velocity
- E = longitudinal dispersion coefficient
- S = rate of surface heat exchange (gain) between water and atmosphere
- ρ = density of water
- c_p = specific heat of water
- h = mean depth of flow
- T = water temperature
- x = distance along the river
- t = time

In the case of rivers, the transport of heat by dispersion is very small as compared to advection and hence can be neglected. Also, since the response of water is slow, a quasi-steady state approach can be used by neglecting the term $\delta T/\delta t$.

Thus equation 2.1 reduces to

$$u \frac{dT}{dx} = \frac{S(T)}{\rho c_p h} \tag{2.2}$$

3. EXCHANGE OF HEAT BETWEEN WATER AND ATMOSPHERE

There is usually exchange of heat between water bodies and the atmosphere. The water bodies lose heat to the atmosphere by back radiation, evaporation, and convection and gain heat primarily through solar radiation and long wave atmospheric radiation. Thus, the net heat transfer can be written as (Stefan et al., 1980)

$$S = H_s - H_\ell - H_e - H_c \tag{3.1}$$

where S = net heat flux

H_s = net shortwave solar radiation entering the water surface

H_ℓ = net longwave radiation leaving the water surface

H_e = energy leaving the water surface due to evaporation, and

H_c = energy conduction/convection from the water to the air

Many different empirical, semi-empirical and deterministic relationships for the terms in equation 3.1 have been developed. The equations which are used in this study are given below.

3.1. NET SHORTWAVE (SOLAR) RADIATION

The magnitude of the solar radiation depends on the altitude of the sun, which varies daily and seasonally for a fixed location on the earth and on the amount of cloud cover. Also, some small part of the incoming solar radiation is reflected at the water surface. The net shortwave radiation is the difference between incoming and reflected radiation and is expressed as

$$H_s = H_{si}(1 - r) \tag{3.2}$$

where H_{si} = incoming solar radiation, and

r = total reflectivity of the water surface.

There are some empirical equations to determine r, but in the present study, it is assumed that the reflectivity of the device measuring solar radiation is equal to that of water surface, so that the measured solar radiation is equal to net solar radiation.

3.2. NET LONGWAVE RADIATION

The net longwave radiation is the difference between the longwave atmospheric radiation and the back radiation from the water surface. It can be expressed as

$$H_{\ell} = \sigma(\varepsilon_w T_s^4 - \varepsilon_a T_a^4) \qquad (3.3)$$

where T_s = water surface temperature (°K),
T_a = air temperature (°K),
ε_w = longwave emissivity of the water surface
$\simeq$ 0.97
ε_a = emissivity of the atmosphere, and
σ = Stefan-Boltzman constant.

The atmospheric emissivity without cloud cover, ε_{ac}, is given by the Idso and Jackson formula.

$$\varepsilon_{ac} = 1 - 0.261 \exp\,[-0.74 * 10^{-4} * T_a^2] \qquad (3.4)$$

where T_a = air temperature in degree Celsius.

The Bolzman formula is then used to find E_a.

$$\varepsilon_a = \varepsilon_{ac}(1 + K\,C_c^2) \qquad (3.5)$$

where C_c = fraction cloud cover, and
K = a coefficient which depends upon cloud height. It varies between 0.04 and 0.25 and an average value of 0.17 is used.

3.3. EVAPORATIVE HEAT TRANSFER

Heat is lost from the water surface to the atmosphere through evaporation from the water. This heat loss is given by the equation

$$H_e = \rho L(Wft_n)(e_{sw} - e_a) \qquad (3.6)$$

where e_a = air vapor pressure,

e_{sw} = saturated vapor pressure at water surface temperature,

Wft_n = wind speed function,

L = latent heat of vaporization for water, and

ρ = density of water.

3.4. HEAT TRANSFER BY CONDUCTION/CONVECTION

This accounts for the loss or gain of heat by the water body by conduction/convection at the air-water interface. It is equal to the product of a heat transfer coefficient and the temperature difference between water surface and air. It can be computed from the following formula derived by Bowen

$$H_c = 0.61 \frac{P_a}{1000} \rho L(Wft_n)(T_s - T_a) \tag{3.7}$$

where T_a = air temperature,

T_s = water surface temperature,

Wft_n = wind speed function, and

P_a = barometric pressure in mb.

4. COMPUTATIONAL METHODS

Three methods for solution of Eq. 2.2 are used. The rate of surface heat exchange S in equation 2.2 is a nonlinear function of the water temperature T. In the first two methods, the term S is approximated by a linear function of T so as to obtain an analytical solution while, in the third method, Eq. 2.2 is solved using numerical integration.

4.1. METHOD BY BRADY, GRAVES, AND GEYER

This method is based on the concept of the equilibrium temperature T_e (Edinger and Geyer, 1965), which is defined as the water surface temperature at which the net heat exchange is zero. The net heat exchange S is then expressed as the product of a surface exchange coefficient K and the temperature difference $(T - T_E)$. Thus,

$$S = - K(T - T_E) \tag{4.1}$$

It follows from the above equation that, for a given set of meteorological conditions, a body of water that has a temperature below equilibrium temperature will approach equilibrium temperature by warming and a body of water above equilibrium temperature will approach equilibrium temperature by cooling.

According to Brady et al. (1969), the surface exchange coefficient K and the equilibrium temperature T_E are determined from the following empirical equations.

$$K = 15.7 + (\beta + 0.26)FW \tag{4.2}$$

where $\beta = 0.255 - 0.0085\ T_w + 0.000204\ T_w^{\ 2}$ (4.3)

$$T_W = \frac{T + T_d}{2} \tag{4.4}$$

where T is the water surface temperature and T_d is the dew point temperature, both in °F.

The wind speed function FW is adapted from the Shulyakovskyi formulation by Ryan and Harleman (1973).

$$FW = 14W + 22.4(\Delta\theta_\nu)^{1/3} \tag{4.5}$$

where FW is in BTU/sqft/day/°F

W = wind velocity in mph, and

$$\Delta\theta_\nu = T(1 + 0.378\ \rho_s/P_a) - T_a(1 + 0.378\ \rho_a/P_a) \tag{4.6}$$

where T = water temerpature in °R,

T_a = air temperature in °R,

P_a = barometric pressure

ρ_s = saturated air vapor pressure at temperature T, and

ρ_a = actual air vapor pressure

$$e_s = 33.8639[(0.00738T + 0.8072)^8 + 0.001316 - 0.000019\ |1.8\ T + 48|] \tag{4.7}$$

$$e_a = 33.8639[(0.00738T_d + 0.8072)^8 + 0.001316 - 0.000019\ |1.8\ T_d + 48|] \tag{4.8}$$

where e_s and e_a are in millibars and T and T_d are in °C. When the first term on the right-hand side of equation 4.6 is less than the second term, $\Delta\theta_\nu$ is set equal to zero.

The equilibrium temperature is given by a relation

$$T_E = T_d + \frac{H_s}{K} \tag{4.9}$$

where H_s = solar radiation received.

Substituting Eq. 4.1 into Eq. 2.2, we get

$$u\frac{dT}{dx} = \frac{-K(T - T_E)}{\rho c_p h} \tag{4.10}$$

The analytical solution to the above equation is given by

$$\frac{T - T_E}{T_o - T_E} = e^{-\frac{x}{u}\frac{K}{\rho c_p h}} \tag{4.11}$$

Substituting u = Q/Bh in equation 4.11, one gets

$$\frac{T - T_E}{T_o - T_E} = e^{-\frac{BxK}{\rho c_p Q}} \qquad (4.12)$$

where x = distance along the river,

T_o = water temperature at x = 0,

B = width of river, and

Q = river discharge.

4.2. METHOD BY PAILY, MACAGNO, AND KENNEDY

In this method, the net heat transfer is approximated by a linear relation of the form

$$S = -(\varepsilon T + \eta) \qquad (4.13)$$

in which η = the base heat exchange rate corresponding to a stream temperature of 0°C,

ε = a heat exchange coefficient, and

T = stream temperature in °C.

The effect of air temperature (T_a), wind velocity (W), and relative humidity (RH) on E and η is shown in Fig. 4.1 and Fig. 4.2, respectively. It can be seen that ε is almost insensitive to changes in relative humidity, especially when the air temperature is very low. However, both ε and η vary significantly with wind velocity and air temperature. Also, these plots are valid for stream temperatures up to only 5°C.

Comparing Eqs. 4.1 and 4.13, we get

$$K = \varepsilon \qquad (4.14)$$

$$T_E = (-\eta/\varepsilon) \qquad (4.15)$$

Equations for ε and η were obtained using Figs. 4.1 and 4.2, respectively. The procedure is described in brief below.

4.2.1. Approximate Equation for ε

Fig. 4.1 shows that ε varies linearly with T_a, so that we can write

$$\varepsilon = a + b(T_a + 1) \tag{4.16}$$

Slope b is constant and a is a function of W and RH. Fig. 4.3(a) shows a as a function of W and RH for $T_a = -1°C$.

From Fig. 4.3(a), we can write

$$a = c + d\,W \tag{4.17}$$

where d is constant and c is a function of RH.

Fig. 4.3(b) shows c as a function of RH for W = 0. Then

$$c = e + f\,RH \tag{4.18}$$

From Eqs. 4.17 and 4.18, a is computed and, when substituted into Eq. 4.16, one obtains the following expression for ε

$$\varepsilon = 30.912 - 1.088\,T_a + 3.1522W - 0.03RH \tag{4.19}$$

4.2.2. Approximate Equation for η

A similar procedure is adapted for obtaining an expression for η. Following Fig. 4.2, one can write

$$\eta = g + h(T_a + 1) \tag{4.20}$$

where both g and h are functions of W and RH. From Figs. 4.4(a), 4.4(b), and 4.4(c), a relation for g is obtained and from Figs. 4.4(d) and 4.4(e), a relation for h is obtained which, after substituting into Eq. 4.20, gives an expression for η as

$$\begin{aligned}\eta = &- 0.00761 * T_a * W * RH - 1.7935 * T_a * W \\ &- 0.03 * T_a * RH - 25.0 * T_a - 0.15921 * W * RH \\ &+ 16.6865 * W - 0.93 * RH - 15.0\end{aligned} \tag{4.21}$$

4.2.3. Accuracy of Eqs. 4.19 and 4.21

The values of ε and η for different sets of meteorological conditions, as reported by Paily et al. (1974), are given in Table 4.1. For the same conditions, ε and η are computed using Eqs. 4.19 and 4.21, respectively, and these are given in Table 4.2. Comparison shows that the error in ε values is less than 0.9% and that in η values is less than

TABLE 4.1. VALUES OF ε AND η IN $S = -(\varepsilon T + \eta)$[a]

Air temperature in degrees Celsius	Wind Velocity in miles per hour (meters per second)	Relative humidity, as a percentage	Base heat exchange rate, η, in calories per square centimeter per day	Heat exchange coefficient, ε, in calories per square centimeter per day per degree Celsius	Correlation coefficient
-1.0	11.0 (4.95)	70.0	33.563	64.835	0.9995
-3.0	11.0 (4.95)	70.0	134.955	67.103	0.9996
-5.0	11.0 (4.95)	70.0	236.802	69.335	0.9996
-10.0	11.0 (4.95)	70.0	494.344	74.778	0.9996
-15.0	11.0 (4.95)	70.0	757.773	80.067	0.9996
-18.0	11.0 (4.95)	70.0	919.190	83.185	0.9997
-5.0	0.0 (0.00)	70.0	47.584	34.422	0.9993
-5.0	3.7 (1.65)	70.0	110.657	46.060	0.9994
-5.0	7.4 (3.30)	70.0	173.729	57.697	0.9995
-5.0	11.0 (4.95)	70.0	236.802	69.335	0.9996
-5.0	14.7 (6.60)	70.0	299.874	80.973	0.9996
-5.0	18.4 (8.25)	70.0	362.947	92.610	0.9997
-5.0	11.0 (4.95)	10.0	354.742	70.719	0.9996
-5.0	11.0 (4.95)	30.0	315.428	70.258	0.9996
-5.0	11.0 (4.95)	50.0	276.115	69.796	0.9996
-5.0	11.0 (4.95)	70.0	236.802	69.335	0.9996
-5.0	11.0 (4.95)	90.0	197.488	68.874	0.9996
-5.0	11.0 (4.95)	100.0	177.832	68.643	0.9996

*Values valid for range of water temperature between 0°C and 5°C; values of other meteorological variables are: barometric pressure = 996.0 mb; cloud height = 3,275 ft (1,000 m); cloud cover = 6; and visibility = 1.87 miles (3km).

TABLE 4.2. COMPUTED VALUES OF η and ε

Air temperature in degrees Celsius	Wind Velocity in miles per hour (meters per second)	Relative humidity, as a percentage	Base heat exchange rate, η, in calories per square centimeter per day	percent error in η	Heat exchange coefficient, ε, in calories per square centimeter per day per degree Celsius	percent error in ε
-1.0	11.0	70.0	33.548	0.045	64.574	0.402
-3.0	11.0	70.0	138.924	-2.941	66.750	0.526
-5.0	11.0	70.0	244.301	-3.167	68.926	0.590
-10.0	11.0	70.0	507.742	-2.710	74.366	0.551
-15.0	11.0	70.0	771.183	-1.770	79.806	0.326
-18.0	11.0	70.0	929.247	-1.061	83.070	0.138
-5.0	0.0	70.0	55.400	-16.426	34.252	0.494
-5.0	3.7	70.0	118.939	-7.485	45.915	0.315
-5.0	7.4	70.0	182.479	-5.036	57.578	0.206
-5.0	11.0	70.0	244.301	-3.167	68.926	0.590
-5.0	14.7	70.0	307.840	-2.657	80.589	0.474
-5.0	18.4	70.0	371.380	-2.323	92.252	0.386
-5.0	11.0	10.0	371.066	-4.602	70.726	-0.010
-5.0	11.0	30.0	328.811	-4.243	70.126	0.188
-5.0	11.0	50.0	286.556	-3.781	69.526	0.387
-5.0	11.0	70.0	244.301	-3.167	68.926	0.590
-5.0	11.0	90.0	202.046	-2.308	68.326	0.795
-5.0	11.0	100.0	180.918	-1.735	68.026	0.899

7% for wind velocities less than 4 mph, the maximum being 16.4% for wind velocity W = 0. However, the error in the net heat transfer S, due to error in η, will decrease as the water temperature increases. For the above case, when W = 0, the error in S will be 6.4% at T = 2°C and 3.2% at T = 5°C.

4.3. NUMERICAL INTEGRATION METHOD

Instead of approximating the net heat transfer S by a linear expression, a numerical integration technique can be used to solve Eq. 2.2. Substituting u = Q/Bh in Eq. 2.2 gives

$$dx = \frac{Q\rho c_p}{BS} dT \qquad \text{or} \tag{4.22}$$

$$dx = f(T)dT \tag{4.23}$$

Using Simpson's formula for numerical integration, one can write

$$dx = \frac{dT}{3}\left[f(T) + f(T + 2dT) + 4f(T + dT)\right] \tag{4.24}$$

where dT = increment in temperature T, and

dx = distance between the points with temperatures T and T + 2dT.

Starting with temperature $T = T_o$ at x = 0 (Dam No. 3), the temperature at the end section of the river can be computed by applying successively Eq. 4.24. The function

$$f(T) = \frac{Q\rho c_p}{BS} \tag{4.25}$$

is computed for each T using Eqs. 3.1 to 3.7.

The windspeed function proposed by Ryan and Harleman (1973) has been used.

$$(Wft_n) = 0.01107 * W + 0.00934(\Delta\theta_\nu)^{1/3}$$

where (Wft_n) is in cm/day/mb

w = wind speed in m/s, and

$\Delta\theta_\nu = T(1 + 0.378\ e_s/P_a) - T_a(1 + 0.378\ e_a/P_a)$

where T and T_a are in °C.

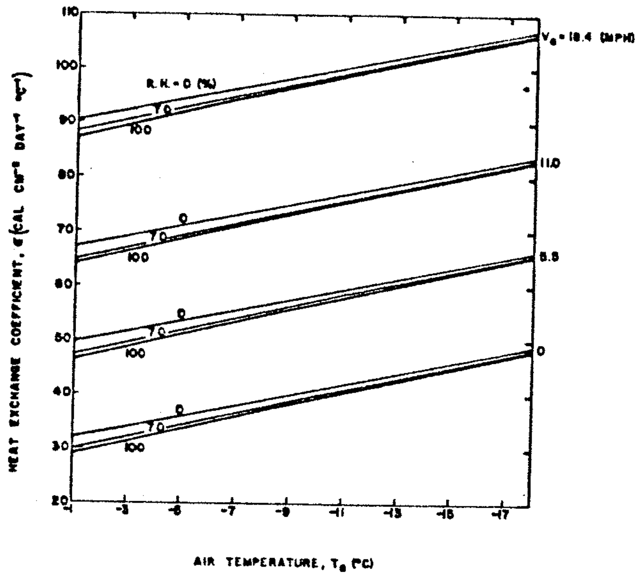

FIG. 4.1 Heat Exchange Coefficient ε as Function of Air Temperature T_a, Wind Velocity V_a, and Relative Humidity RH

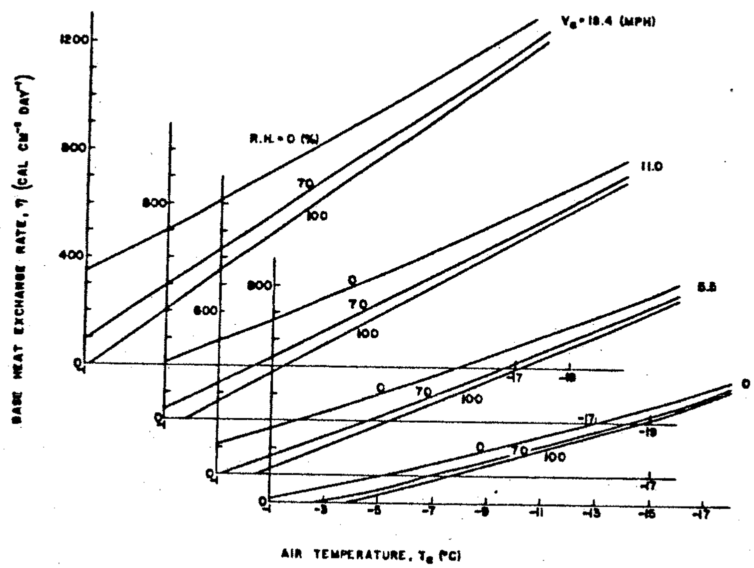

FIG. 4.2 Base Heat Exchange Rate η as Function of Air Temperature T_a, Wind Velocity V_a, and Relative Humidity RH

(after Paily et al, 1974)

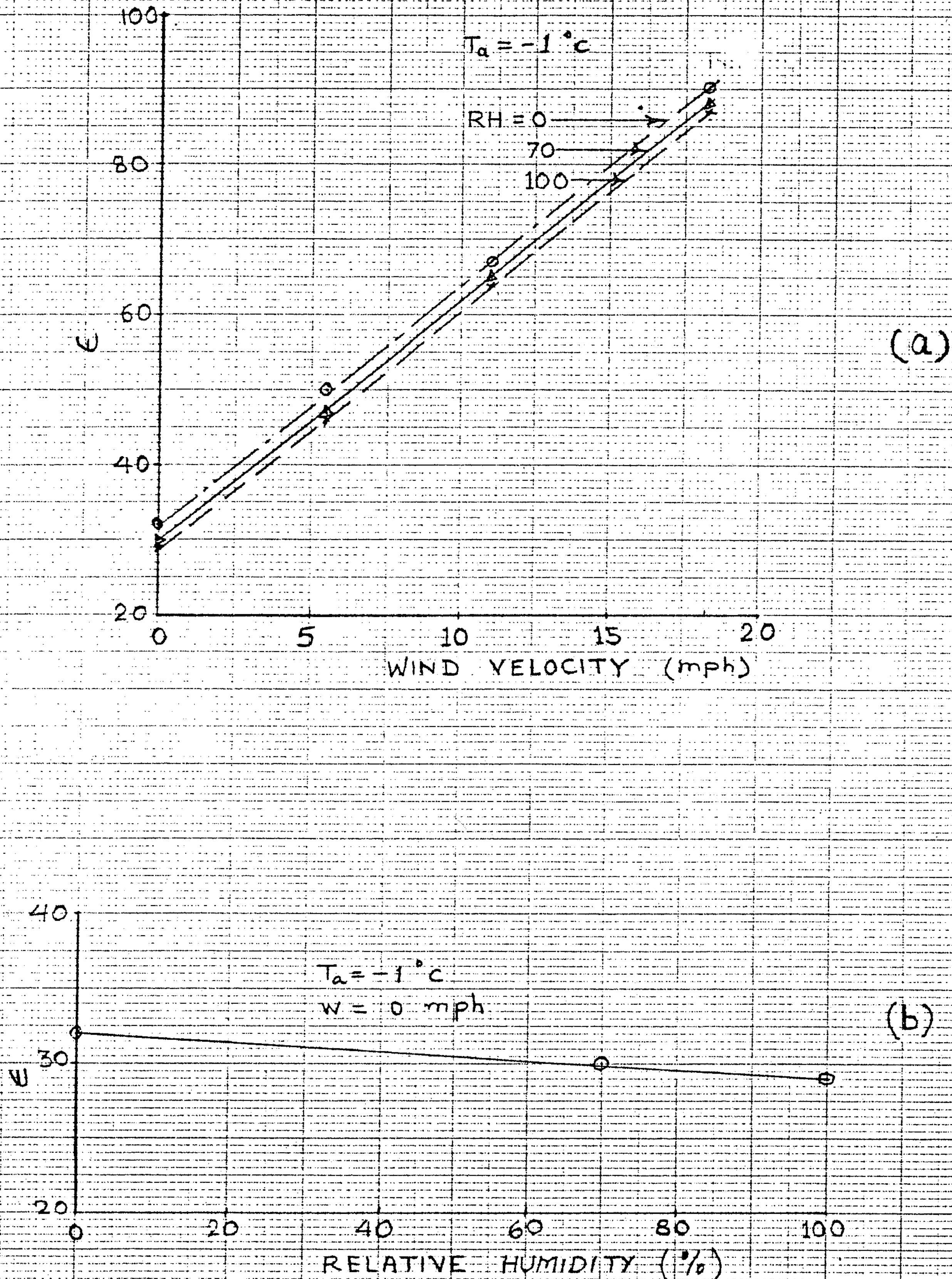

FIG. 4.3 VARIATION OF HEAT EXCHANGE COEFF. WITH WIND VELOCITY & REL. HUMIDITY

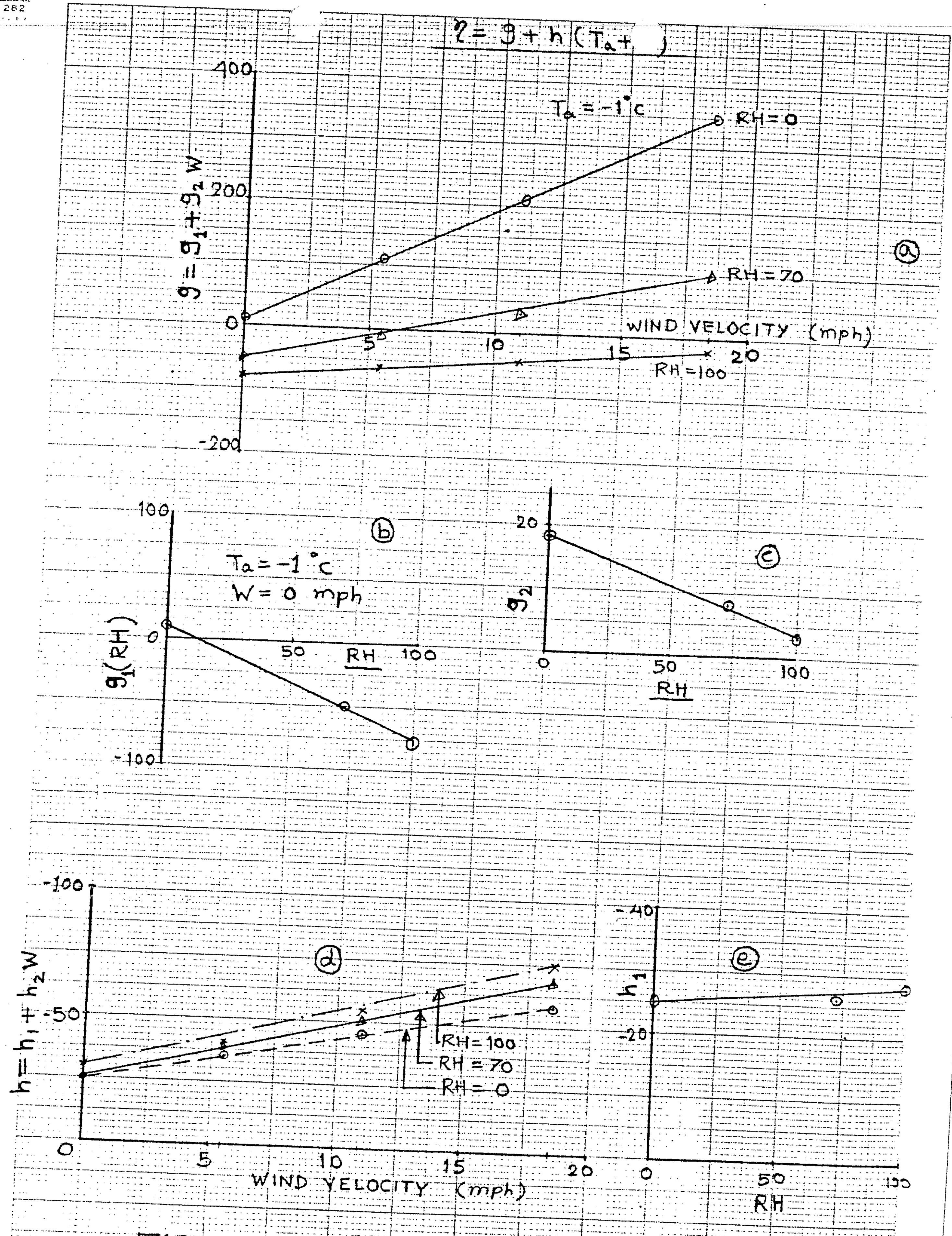

FIG. 4.4 VARIATION OF BASE HEAT EXCHANGE RATE η WITH WIND VELOCITY AND RELATIVE HUMIDITY

5. INPUT DATA

5.1. MISSISSIPPI RIVER GEOMETRY

The methods described in the previous section were used to predict water temperatures in the Mississippi River. The river reach between Lock and Dam No. 3 and Lake Pepin was considered. The river configuration in this reach is schematically shown in Fig. 5.1. The river divides into two channels about 3 miles downstream of Dam No. 3. The geometry of the three channels of river is given in Table 5.1. The total discharge Q in the upstream mainstream is distributed in the two downstream channels according to a relation given by Stefan (1980) as

$$Q_m = 0.0000041Q^2 + 0.5437Q + 1195.94 \tag{5.1}$$

$$Q_w = Q - Q_m \tag{5.2}$$

where Q_m = discharge in the downstream mainstem channel, and
Q_w = discharge in the Wisconsin channel.

The Prairie Island Nuclear Power Generating Plant is located on the Mississippi River just upstream from Dam No. 3. The plant withdraws cooling water from the Mississippi River. The full heat discharge from the plant is approximately 8.34×10^9 BTU/hr (580,000 Kcal/s). To evaluate heat input on water tempueratures in the winter season, prediction of water temperatures was made at the end of the reach, where the two channels join Lake Pepin.

5.2. METEOROLOGICAL AND RIVER FLOW DATA

The analysis of water temperatures was made for the period December 1 to March 31 for the years 1981 to 1986.

The required climatological data, such as average air temperatures, average dew point temperature, average wind speed, and sky cover, were taken from the data published by the National Oceanic and Atmospheric Administration. The above data was for Minneapolis-St. Paul, which is about 35 miles upstream of Dam No. 3. The only data which was available for the area in the vicinity of Dam No. 3 was average air temperatures at Red Wing. These were plotted against the temperatures at Minneapolis-St. Paul, as shown in Fig. 5.2. It can be seen from the figure that the air temperatures at Red Wing are quite close to those at Minneapolis-St. Paul. Hence, all the climatological data for Minneapolis-St. Paul were used.

The average daily solar radiation was obtained from Professor Donald G. Baker, Soil Science Department, St. Paul Campus, University of Minnesota.

TABLE 5.1. SUMMARY OF RIVER GEOMETRY

	Length	Ave. Width	Total Surface Area	Average Depth at 10,000 cfs
	(mi)	(ft)	(sq mi)	(ft)
Upstream Mainstem	3.04	800	0.461	11.7
Downstream Mainstem	8.0	730	1.106	11.7
Wisconsin (North) Channel	6.8	620	0.798	6.8

The daily river flow and the average water temperatures at Dam No. 3 were taken from the reports of the Environmental and Regulatory Activities Department, Northern States Power Company. However, for the period Dec. 1981 to Dec. 1982, the water temperatures at Dam No. 3 were not available. For that period, the inlet water temperatures and the water temperatures downstream of the plant at point 'A' in the channel, as shown in Fig. 5.3, were available. According to the studies made by Stefan and Anderson (1980), the flow in the channel was taken approximately equal to 10% of the river flow, and the water temperatures at Dam No. 3 were estimated using that flow ratio. For the month of December 1982, the water temperature data were not reliable and hence no computations were made for that particular month.

The data used in this study is given in Appendix A.

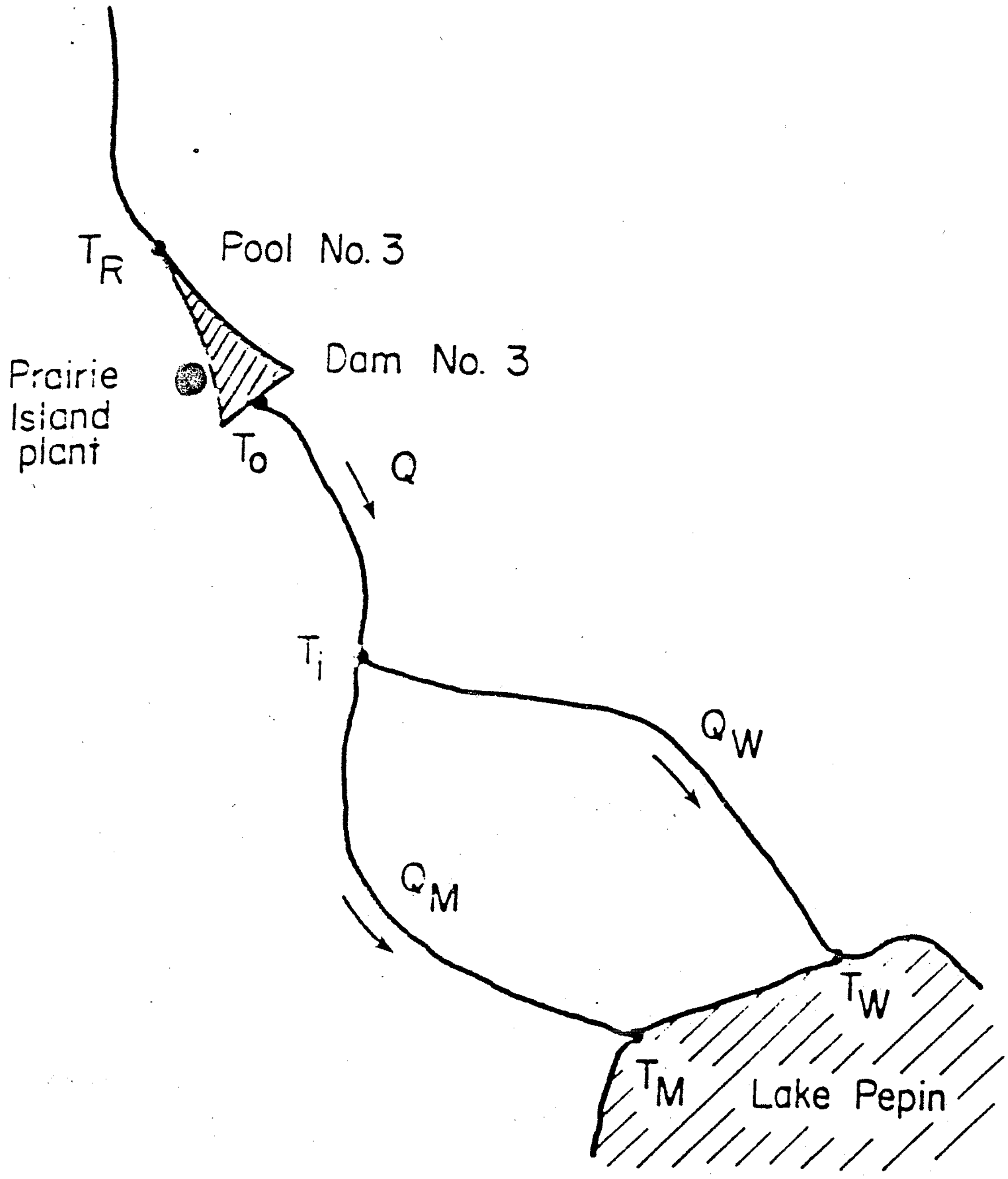

FIG. 5.1 SCHEMATIC OF MISSISSIPPI RIVER SYSTEM FOR WATER TEMPERATURE ANALYSIS.

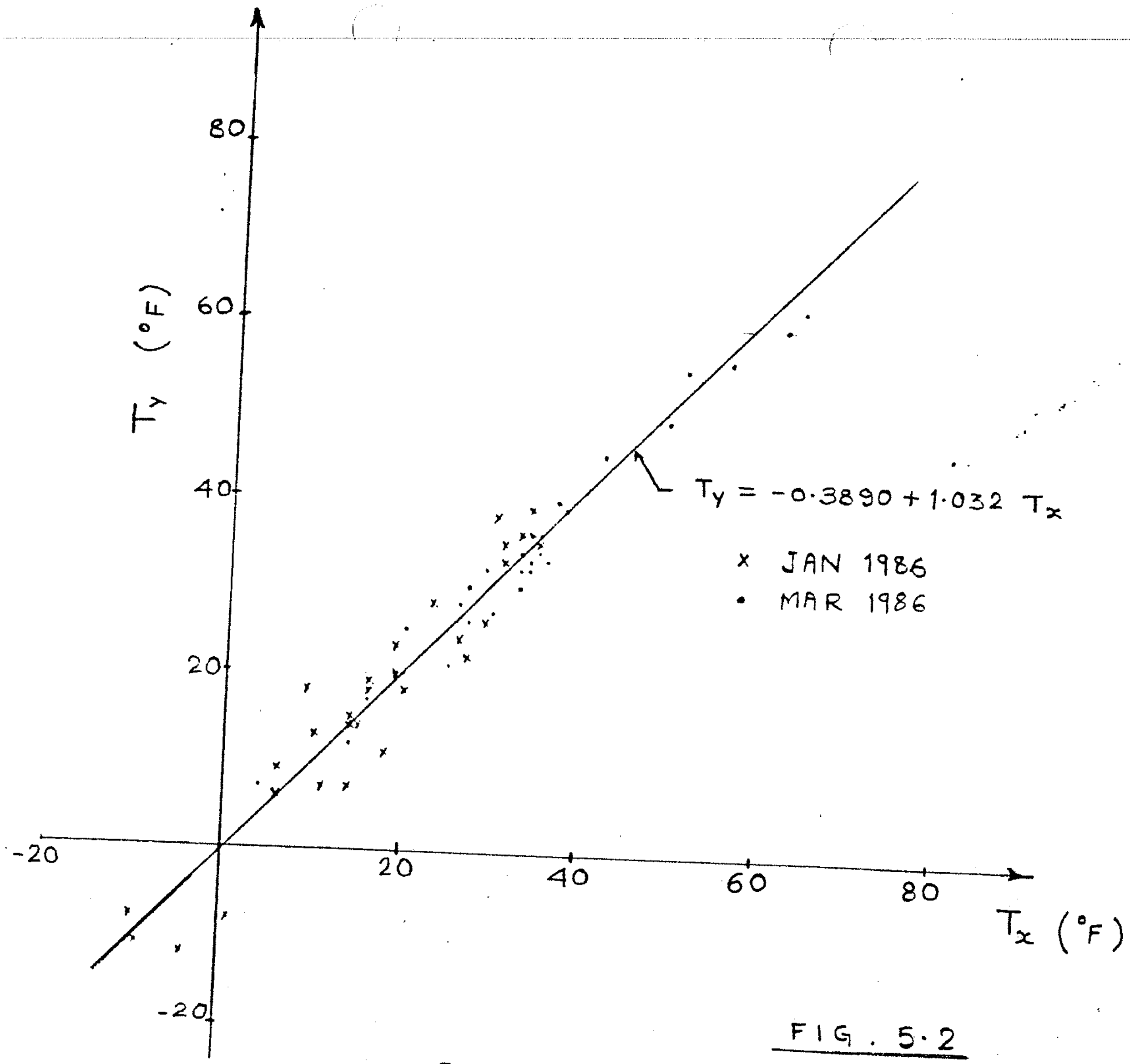

FIG. 5·2

PLOT OF AIR TEMP. AT RED WING (T_y) VERSUS AIR TEMP. AT MINNEAPOLIS - ST. PAUL (T_x)

RTD (Resistance Temperature Device) Locations at Prairie Island Nuclear Generating Plant.

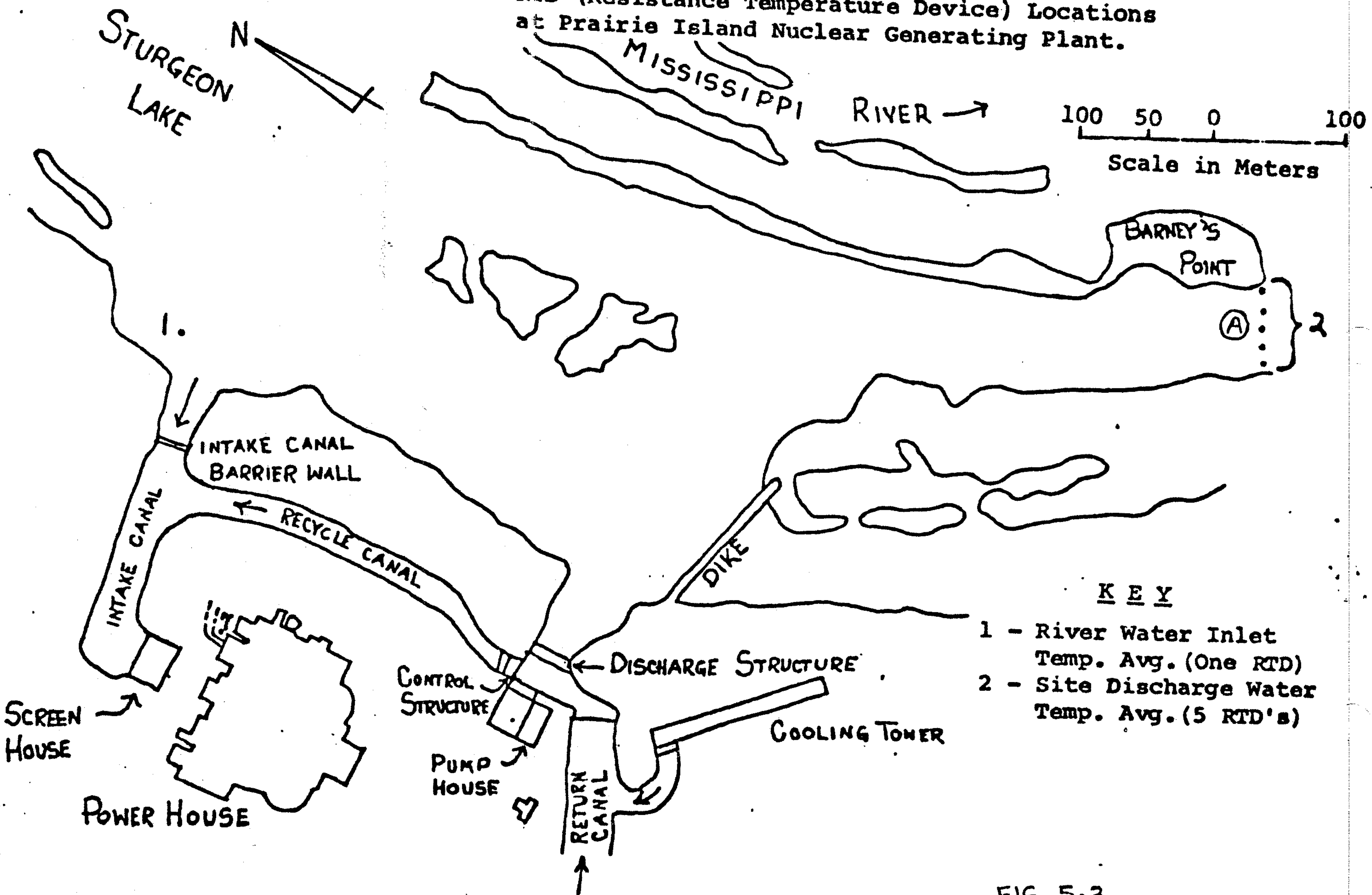

FIG. 5-3

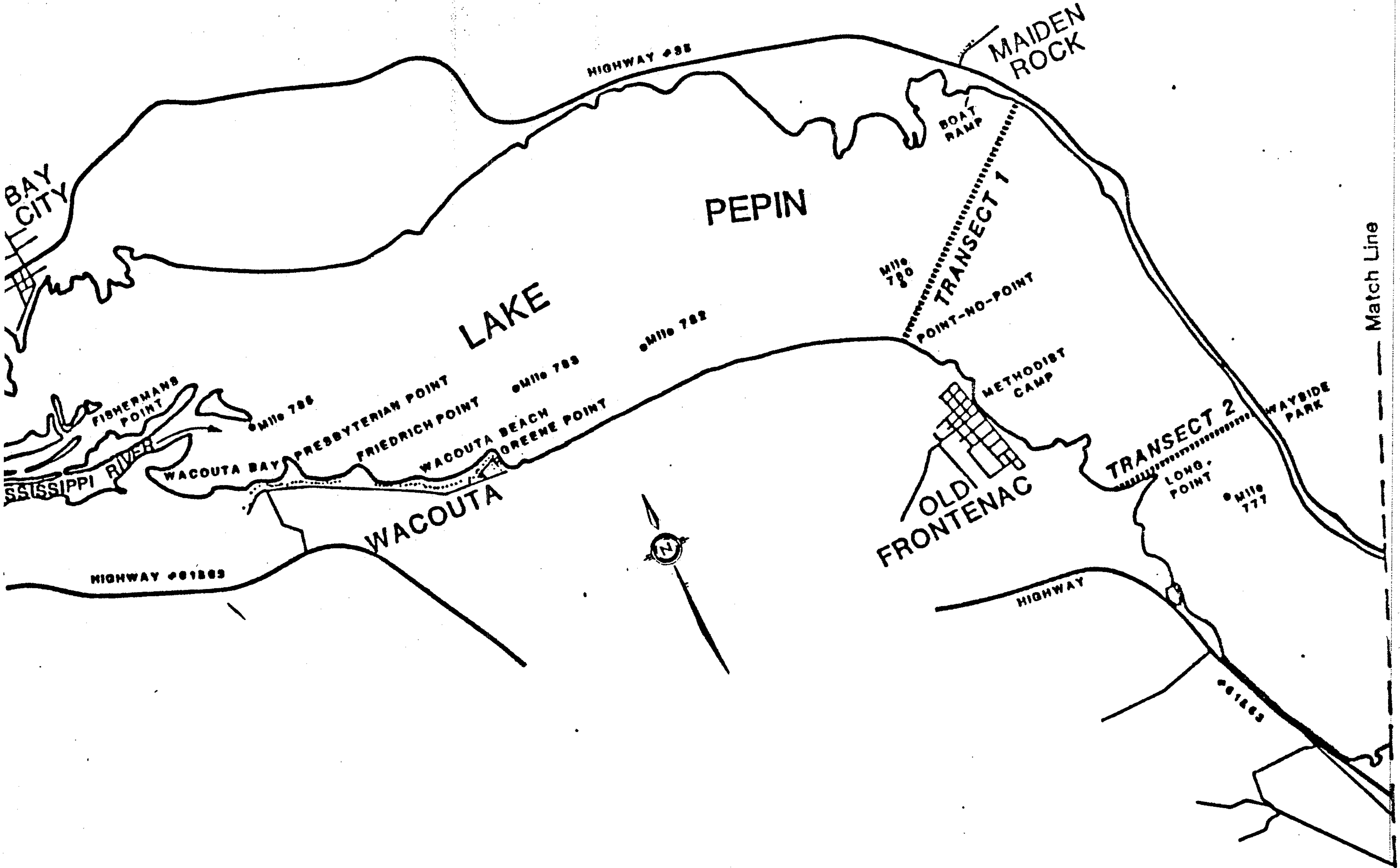

FIG. 5.4 LAKE PEPIN - PLAN VIEW

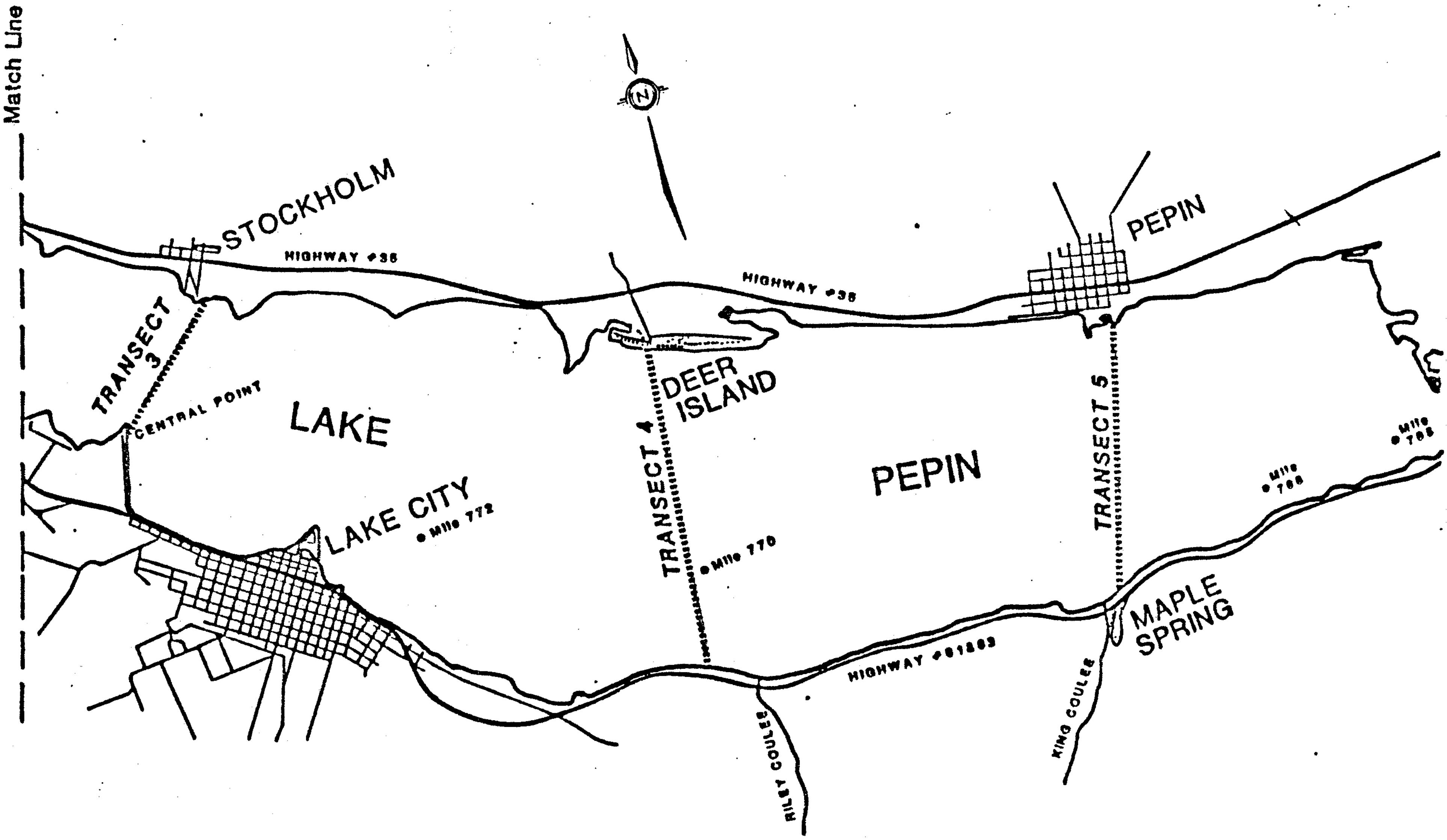
Match Line
STOCKHOLM
HIGHWAY #35
HIGHWAY #35
PEPIN
TRANSECT 3
CENTRAL POINT
LAKE
LAKE CITY
Mile 772
TRANSECT 4
DEER ISLAND
Mile 770
PEPIN
TRANSECT 5
MAPLE SPRING
RILEY COULEE
KING COULEE

Fig. 5.4 (cont'd)

6. RESULTS

6.1. COMPUTATION OF WATER TEMPERATURES IN THE MISSISSIPPI RIVER AT THE INFLOW TO LAKE PEPIN

A computer program was written to predict the water temperatures T_m and T_w at the downstream end of the river reach using the three methods described. The program is given in Appendix B and the results are given in Appendix C.

Since the formulation of the second method was based exclusively on winter conditions, the results obtained by the other two methods are compared with those obtained by the second method. The temperatures T_m obtained by using method 1 and method 2, for December 1985 to March 1986, are plotted as shown in Figs. 6.1(a) to Fig. 6.1(d). Similar plots are prepared for comparison of method 3 and method 2, as shown in Figs. 6.2(a) to 6.2(d). The temperatures obtained by method 1 are slightly higher for December and January and slightly lower for February and March than the temperatures obtained by method 2. Method 3 predicted somewhat lower temperatures than method 2 for all four months. However, the difference between the temperatures is not more than ± 0.5°C.

As already mentioned, the water temperature at the downstream end depends on the weather, as well as on the artificial heat input. To separate the two effects, further analysis was made using the results obtained by method 2.

The temperatures T_m and T_w were plotted against (T_o*Q) as shown in Figs. 6.3 through 6.10. The product T_oQ is a measure of the total heat flow carried by the river at Dam No. 3. If multiplied by specific heat ρc_p = 1000 Kcal m^{-3} $°C^{-1}$ the units of $T_oQ\rho c_p$ are Kcal/sec. A necessary but not sufficient condition to indicate that the plant was working at full capacity is $T_oQ > 580$ (°C m^3/s). The number of days for different temperature ranges are also shown in the above figures. A trend indicates that the temperature increases as (T_o*Q) increases, but the scatter which is due to the variable weather conditions is very large. The relation between the heat content at Dam No. 3 and the water temperature at the inflow to Lake Pepin depend very strongly on weather.

A frequency analysis of T_m and T_w was made and the average number of days are plotted against (T_o*Q) for different ranges of temperatures. These are shown in Figs. 6.11 and 6.12. It is readily apparent that higher inflow temperatures T_m to Lake Pepin require on the average higher heat flows to T_oQ at Dam No. 3. More importantly it is also apparent in Figs. 6.11 and 6.12, that elevated inflow temperatures to Lake Pepin (e.g. T_m = 0.5 to 1.0°C) can occur over a very wide range of heat flows at the dam (T_oQ from 300 to 1200 (°C m^3/s) in this example). One may interpret this to mean that weather has a very important influence on the control of inflow water temperatures to Lake Pepin.

Another way of plotting the data is derived from Eq. 4.12 which, after expanding the right hand side in a series and rearranging, can be written in the form

$$T = T_o * f_1 + f_2 \qquad (6.1)$$

Both f_1 and f_2 are functions of weather parameters and river flow. In accordince with Eq. 6.1, the temperatures T_m are plotted against T_o for December 1985 to March 1986 as shown in Fig. 6.13. Because of large scatter with weather, it is not possible to obtain any unique relation between T_m and T_o in the above form.

The monthly mean and standard deviations of the temperatures T_o, T_m, and T_w were computed. They are given in Table 6.1. Figure 6.14 shows a plot of $\overline{T}_m$ against $\overline{T}_o$ for different months. Standard deviations of T_m and T_o are also plotted. It can be seen that $\overline{T}_m$ increases as $\overline{T}_o$ increases. A straight line is fitted approximately to obtain the temperature $(\overline{T}_o)_{min}$ for each month. $(\overline{T}_o)_{min}$ is the minimum temperature to have nonzero average inflow temperature $\overline{T}_m$ to Lake Pepin. $(\overline{T}_o)_{min}$ values are plotted and a curve is drawn as shown in the same figure. The period between the points where the curve cuts the time axis, namely approximately November 26 to April 7, represents the cooling period during which average river temperatures would be at freezing and the remaining period is on average the warming period. An individual days inflow temperature to Lake Pepin may be as much as 2°C above the average in midwinter as shown in Fig. 6.14.

6.2. Effect of residual heat input at the head of Lake Pepin on ice cover

The residual heat content in the Mississippi River water may affect the ice cover on Lake Pepin. The effect of residual heat on the ice cover was first studied in a very simplistic way. From the computed temperatures T_m and T_w ice cover free-area of the lake was determined using Eq. 4.12. In the deviation of Eq. 4.12, it is assumed that the temperature across the section is uniform. However, when the river enters the lake the warm flow is plunging and hence the assumption of uniform temperature across the cross section is not valid. Thus, these results give an incorrect picture of the effect of residual heat on the ice cover.

7. EXPECTATIONS FOR STRATIFIED FLOW OF RIVER WATER THROUGH LAKE PEPIN IN WINTER AND EFFECT ON ICE COVERS

7.1. CONCEPTS

The effects of slightly elevated water inflow temperatures to Lake Pepin can only be evaluated qualitatively at this time. The water temperature profiles measured by Northern States Power Company in winter under the ice of Lake Pepin show an inverse stratification. The water temperature changes from 0°C at the underside of the ice to temperatures in the vicinity of 1°C at greater depth. This follows typical lake temperature stratification patterns found in Minnesota lakes and is directly related to the relationship between density and temperature of water between 0°C and 4°C (density increases with temperature). In that range a stable stratification requires warmer water to move to a depth greater than that for colder water. This is important for Lake Pepin because it means that the warmer Mississippi River inflow will tend to form an interflow through the lake at a greater depth, hence further away from the ice cover. This simplistic picture is unfortunately rendered more complicated by vertical mixing induced by the flow through the lake. The movement of the river water as an interflow (layer of unknown thickness at some intermediate depth) generates some vertical turbulent mixing which will tend to carry eddies of warm water upwards towards the underside of the ice. If this additional heat flux can be conducted away through the ice cover to the atmosphere, the ice thickness will not be affected. At this time the turbulence generated by the slow interflow in a very weakly density-stratified lake has not been assessed, and the stratified flow and heat transfer rates in Lake Pepin have not been quantified.

7.2. POSSIBLE SIMULATION OF VERTICAL PROFILES OF WATER TEMPERATURE IN LAKE PEPIN

To obtain at least an idea of winter temperature stratification dynamics at Lake Pepin, vertical profiles of temperature in the Lake were simulated using the computer model RESQUAL II. This is a one-dimensional lake temperature stratification model developed for summer conditions. The lake is considered to be composed of horizontal layers of variable thickness and density. The density of each layer is determined by its temperature. The inflowing water will seek a layer with a density equal to its own. It will augment the volume of that layer and consequently all the layers above it will be displaced upward. If the density of the inflow water is higher, it will behave as a plunging flow and will entrain water from each layer it passes through. The amount of entrainment is a complex function of the flow rate, the density gradients, and other factors.

Lake Pepin is about 35 km long, 2.9 km wide, and the maximum depth is 12.2 m. The following expressions were used to compute the area and volume of the lake at various depths (m^2):

$$\text{Area} = 0.694 \times 10^6 \text{ ZD} \qquad \text{ZD} < 3.05 \text{ m}$$
$$= 2.117 \times 10^6 + 16.54 \times 10^6 (\text{ZD} - 3.05) \qquad 3.05 < \text{ZD} < 6.1 \text{ m}$$
$$= 52.57 \times 10^6 + 7.762 \times 10^6 (\text{ZD} - 6.1) \qquad \text{ZD} > 6.1 \text{ m}$$
$$\text{Volume } (m^3) = 0.2 \times 10^5 (\text{ZD})^{4.65} \qquad \text{ZD} < 6.1 \text{ m}$$
$$= 0.691 \times 10^6 (\text{ZD})^{2.689} \qquad \text{ZD} > 6.1 \text{ m}$$

The dimensions of the inlet and outlet channels are given below:

Inlet channel:

width	= 410 m
bed slope	= 1/400
roughness coefficient	= 0.03

Outlet channel:

bottom width	= 457.2 m
side slope	= 90°
bottom elevation	= 198.7 m

The inflow to the lake is given by the addition of the discharges in the mainstem and the Wisconsin channel. The temperature of inflow was computed by averaging the temperatures T_m T_w obtained in the first part of the study. Field data for vertical profile of temperature was available for a few days at five cross sections along the lake. From this data it was observed that there was ahorizontal temperature gradient with higher temperature water near banks. Hence the data for five sections was averaged to obtain one representative profile. Since no temperature field data was available for November 30, an initial condition for all layers at 0°C was assumed. The vertical turbulent diffusion coefficient was taken equal to 1.0 m^2/day.

In winter Lake Pepin is usually ice covered, and hence heat will be transferred across the surface by conduction only. The rate of heat transfer will depend on the air temperature and the ice cover thickness. In the simulations, it was assumed that there is no heat transfer across the surface.

Vertical water temperature profiles were simulated for the period from December 1985 to March 1986. The computed temperature profiles showed an inverse temperature stratification much as the measured ones, but did not fully agree with the measurements. The main reason for the difference is probably the assumption of zero heat transfer at the water surface.

The preliminary simulation results support the idea that the Mississippi River inflow at elevated temperatures passes through Lake Pepin as an interflow.

The ice thicknesses measured between 1981 and 1986 indicate that the interflow does not affect the ice cover very adversely. However, the heat load to the river from the powerplant was not maximum in all those years. Heat loads at lock and dam No. 3 indicate that in January/Februry 1984 and 1986 heat rejection was maximum while in January/February 1982 and 1985 it was much below maximum capacity. The ice cover did not seem to respond strongly to these differences.

8. CONCLUSIONS AND RECOMMENDATIONS

This study has shown that on the average the Mississippi River inflow to Lake Pepin will have water temperatures above 0°C in winter when river temperatures at dam No. 3 are higher than 0.4°C in December, 0.7°C in January, 0.5°C in February, and 0.2°C in March (Fig. 6.14). When the Prairie Island plant is working at full capacity in a once-through cooling water cycle, the heat rejection from the plant produces river water temperatures at dam No. 3 which are higher than the above values, and therefore a residual heat input to Lake Pepin occurs. The 1985/86 data in Table 6.1 can give an idea. An average relationship between inflow water temperatures to Lake Pepin (T_m) and river temperatures at dam No. 3 (T_o) is shown in Fig. 6.14 for each winter month.

On any particular day actual lake inflow temperatures T_m may deviate greatly from the average value because of the very strong influence of meteorological parameters on the heat transfer between a water surface and the atmosphere. The range of daily inflow water temperatures to Lake Pepin which occurred in the winters of 1981/82 to 1985/86 is documented by this study (Figs. 6.3 to 6.10). Inflow temperatures are given for both the main channel (T_m) and the Wisconsin channel (T_w).

The frequency of occurrence of inflow water temperatures in ranges (increments) of 0.5°C is also shown. The wide range of possible inflow temperatures T_m and T_w which is readily apparent in Figs. 6.3 to 6.10 is caused by both variations in heat load carried by the river at dam No. 3 and by variations in weather. To account for the upstream heat load all water temperatures have been plotted against ($Q\ T_o$). The remaining scatter must be due to weather variations, and it is very significant.

A summary of the frequency distributions for all five winters investigated is given in Fig. 6.11. The effects of upstream heat input and weather are apparent.

Heat rejection from the plant at full capacity represents a value $T_o{*}Q \approx 600(°C\ m^3/s)$. During the winters analyzed plant heat rejection has ranged from zero or near zero (January/February 1982 and 1985) to full capacity or near full capacity (January/February 1984 and 1986). Therefore the full range of possible conditions with regard to heat loads has been investigated, and the range of residual heat inputs to Lake Pepin has been established.

How does the ice cover on Lake Pepin then respond to this input. A detailed analysis of this question was beyond the scope of this study. However, a few findings and thoughts can be presented.

The ice thicknesses measured on Lake Pepin do not seem to respond to the large variations in residual heat input. A further analysis of this point is necessary, and the 1986/87 data may prove to be the most useful for such an analysis. The vertical lake temperature structure underneath the ice would require the river inflow to pass through Lake Pepin as an interflow, i.e. a stratified flow at some intermediate depth. A very crude simulation of the temperature stratification dynamics in Lake Pepin during the winter months indicates that such a flow exists.

The data on ice thicknesses and water temperatures in Lake Pepin which have been collected by Northern States Power Company (NSP) until 1987 are sufficient to analyze the effects of residual heat input to the lake. Therefore, the data collection can be discontinued. NSP should analyze the data and develop a more complete understanding of flow and heat transfer processes in Lake Pepin under winter conditions, and the effects of residual heat inputs on those flows.

NSP should continue to put warning signs around the shores of Lake Pepin against possible ice weaknesses.

REFERENCES

1. Brady, D. K., Graves, W. L. and Geyer, J. C., "Surface Heat Exchange at Power Plant Cooling Lakes," Research Project Report PR 4905, Johns Hopkins University, Dept. of Geography and Environmental Engineering, 1969.

2. Paily, P. P., Macagno, E. O., and Kennedy, J. R., "Winter-Regime Thermal Response to Heated Streams," Jour. of Hydraulic Division, ASCE, Vol. 100, No. HY4, April, 1974.

3. Ryan, P. J. and Harleman, D.R.F., "An Analytical and Experimental Study of the Transient Cooling Pond Behavior," Parsons Laboratory for Water Resources and Hydrodynamics Report No. 161, Massachusetts Institute of Technology, January 1973.

4. Stefan, H. and Anderson K. J., "Wind Driven Flow in Mississippi River Impoundment," Jour. of the Hydraulic Division, ASCE, Vol. 106, HY9, September, 1980.

5. Stefan, H., "Mississippi River Ice Cover Between Dam No. 3 and Lake Pepin," Project Report No. 191, St. Anthony Falls Hydraulic Laboratory, University of Minnesota, June 1980.

6. Stefan, H. G., Gulliver, J., Hahn, M. G. and Fu, A. Y., "Water Temperature Dynamics in Experimental Field Channels: Analysis and Modelling," Project Report No. 193, St. Anthony Falls Hydraulic Laboratory, University of Minnesota, June 1980.

7. Edinger, J. E. and Geyer, J. C., "Heat Exchange in the Environment," Research Project Report PR49, Johns Hopkins University Sanitary Engineering and Water Resources Dept., June, 1965.